Available online at www.sciencedirect.com
SCIENCE DIRECT®
Catalysis Today 93–95 (2004) 619–626
CATALYSIS TODAY
www.elsevier.com/locate/cattod

Synthesis and characterization of carbon black supported Pt–Ru alloy as a model catalyst for fuel cells

Yao Jun Zhang [a,1], A. Maroto-Valiente [a], I. Rodriguez-Ramos [a], Qin Xin [b], A. Guerrero-Ruiz [c,*]

[a] *Instituto de Catálisis y Petroleoquímica, CSIC, Campus Cantoblanco, 28049 Madrid, Spain*
[b] *Dalian Institute of Chemical Physics, Chinese Academy of Science, PR China*
[c] *Departamento de Química Inorgánica y Técnica, Facultad de Ciencias, UNED, Senda del rey s/n, 28040 Madrid, Spain*

Available online 3 July 2004

Abstract

A set of bimetallic Pt–Ru catalysts prepared by co-impregnation of carbon black with ruthenium(III) chloride hydrate and hydrogen hexachloroplatinate(IV) hydrate were investigated by temperature-programmed reduction (TPR), chemisorption of hydrogen, transmission electron microscopy (TEM), microcalorimetry of adsorbed CO and a structure-sensitive reaction (*n*-hexane conversion). The results showed that the volumetric capacities for CO and H_2 adsorption is influenced in the bimetallic Pt–Ru catalysts by the formation of a Pt–Ru alloy. The *n*-hexane reaction revealed that the reaction mechanism for the pure Pt catalyst mainly occurs via cyclic isomerization and aromatization due to the presence of bigger Pt surface ensembles, whereas the Pt–Ru catalysts exhibited predominantly bond-shift isomerization by the diluting effect of Ru metal addition. The differential heats of CO chemisorption on Pt–Ru catalysts fell between the two monometallic Pt and Ru catalysts extremes.

Keywords: Carbon black; Pt–Ru alloy catalysts; Temperature-programmed reduction; Adsorption of H_2 and CO; *n*-Hexane; Differential heats of adsorption; Microcalorimetry

1. Introduction

Carbon supported bimetallic platinum catalysts have been widely studied as anode catalysts for low temperature polymer electrolyte membrane fuel cells (PEMFCs) [1,2] and for direct methanol fuel cells (DMFCs) [3]. CO poisons monometallic platinum electrodes at a concentration as low as 10 ppm and lowers PEMFCs output power by 50%. Alloy of Pt with other metals, such as Ru, Sn or Mo, is known to provide more CO-tolerant anodes with better performance.

Up to now, carbon supported Pt–Ru system has been considered to be the best candidate for CO tolerance at the anode of PEMFCs [4] and for electrochemical oxidation of methanol at anode of DMFCs [5], even though many other promoting agents in conjunction with platinum were reported [6–8]. To further improve the electrocatalytic properties of Pt–Ru bimetallic system, many researchers focused their attention on: (i) developing much more CO-tolerant catalysts with appropriately atomic ratios of Pt–Ru alloy, (ii) preparing highly dispersed catalysts to maximize the active metal surface area, (iii) decreasing noble metal loading as much as possible, (iv) modifying the surface composition by adding second or third promoters and (v) choosing suitable supports.

The electrocatalytic activity of the Pt–Ru catalysts has been proposed to proceed via a "bifunctional effect" in which Ru sites adsorbs oxygen-containing species and give rise to oxidation of the CO adsorbed at the Pt sites [9]. Also an "electronic effect" in which Ru alters the electronic properties of Pt in the alloy formed between the two metals has been postulated [10]. An atomic ratio of Pt to Ru of 1:1 was found to be the best chemical composition for the most CO-tolerant anode catalyst [10]. Many papers dealing with the synthesis of this kind of catalysts using co-impregnation and colloidal methods can be found in the recent literature [11–14]. But to our knowledge, little attention has been paid to the characterization of carbon supported Pt–Ru catalysts [15].

* Corresponding author. Tel.: +34 91 5857965; fax: +34 91 5854760.
E-mail address: aguerrero@ccia.uned.es (A. Guerrero-Ruiz).
[1] On leave from Department of Chemical Engineering, Shiyou University, Shaanxi, PR China.

0920-5861/$ – see front matter © 2004 Elsevier B.V. All rights reserved.
doi:10.1016/j.cattod.2004.06.017

In order to further understand the chemical behavior of the bimetallic Pt–Ru system, we have performed a study of its surface properties. A series of carbon black (Vulcan XC72R) supported Pt–Ru catalysts with 2 wt.% Pt loading and with different weight percentages of Ru were prepared. The atomic ratios of Pt to Ru were adjusted to values of 2:1, 1:1 and 1:2. Several characterization techniques including H_2 and CO chemisorption, temperature-programmed reduction (TPR), transmission electron microscopy (TEM), *n*-hexane isomerization reaction and CO adsorption microcalorimetry were used to characterize the bimetallic Pt–Ru catalysts in order to provide some information about interactions among the two metals and the support surface, dispersion of active species, magnitude of particle sizes, formation of Pt–Ru alloys. This study can provide a fundamental knowledge on the surface properties of these bimetallic systems, which can be further used to develop highly dispersed bimetallic Pt–Ru catalysts for effective fuel cells anodes.

2. Experimental

2.1. Support

A commercial powdered carbon black (VULCAN XC72R, Cabot. Corp., $S_{BET} = 135\,m^2\,g^{-1}$) was used as support of the catalysts. The characterization of the porous texture of the XC72R and the determination of the specific surface area were carried out by physical adsorption of N_2 at 77 K in a Micromeritics TRISTAR 3000. An amount of 0.3 g of catalyst was put into a glass tube and outgassed under vacuum at 523 K for 20 h. Then, the isotherm for N_2 adsorption was carried out at the temperature of liquid N_2.

Oxygen surface groups of carbon support were determined by thermogravimetric analysis (Microbalance CI Electromics Model MK2-MC5) in a flow of helium of $20\,ml\,min^{-1}$ heating from room temperature up to 973 K with a heating rate of $5\,K\,min^{-1}$. A more detailed description of the experimental setup is described elsewhere [16].

2.2. Preparation of catalysts

Platinum–ruthenium catalysts were prepared by incipient wetness co-impregnation of the carbon support with solutions of $RuCl_3{\cdot}xH_2O$ (Aldrich) and $H_2PtCl_6{\cdot}6H_2O$ (Aldrich) in a benzene and ethanol mixture (4:1 in volume) [17] with the appropriate concentrations to obtain different loadings: 2 wt.% Pt–0.52 wt.% Ru, 2 wt.% Pt–1.03 wt.% Ru and 2 wt.% Pt–2.03 wt.% Ru with atomic ratios of Pt to Ru of 2:1, 1:1 and 1:2, respectively. Monometallic catalysts of platinum and ruthenium were prepared by the same method with an appropriate concentration of noble metal salts to get loadings of 2 wt.% Pt and 2 wt.% Ru, respectively. The samples were dried at room temperature for 48 h and then placed in an oven at 398 K for 8 h under air atmosphere.

2.3. Characterization of catalysts

Temperature-programmed reduction experiments were carried out in an apparatus equipped with a mass flow controlling system. Sample of 0.35 g was placed between two quartz wool plugs in a U-shaped quartz reactor. A mixture of 12 vol.% hydrogen in helium was fed into the reactor at a total flow rate of $22\,ml\,min^{-1}$. Before beginning the experiments, helium was passed through the reactor for 2 h to flush the system and then the sample was heated from room temperature up to 1023 K at a rate of $5\,K\,min^{-1}$. The effluents were monitored by a gas chromatograph (Varian 3400) equipped with a thermal conductivity detector. The effluents were automatically injected at intervals of 3.5 min.

Hydrogen chemisorption measurements were performed in a conventional volumetric system. Sample of 0.1 g was placed in a quartz reactor connected to a vacuum system and evacuated overnight at room temperature. Sample was heated from room temperature to 573 K, reduced for 2 h under H_2 and outgassed at 673 K for 1 h. Then, the sample was cooled to room temperature and chemisorption measurements were performed. Hydrogen uptakes were determined by extrapolation of the linear part of the isotherm to zero pressure.

CO adsorption with simultaneous measure of the evolved heats was determined in a differential heat-flow microcalorimeter of the Tian-Calvet type (C80-II from Setaram) at 330 K [18]. A glass adsorption vessel containing 0.2 g of sample was linked to a volumetric apparatus, which permitted the introduction of successive small pulses of CO. The equilibrium pressure was measured by means of capacitance manometers (MKS Baratron model 627). The catalyst was reduced in situ at 573 K for 2 h under a H_2 flow of $43\,ml\,min^{-1}$ and outgassed at 673 K for 16 h. The sample was then cooled down to 330 K and successive doses of CO were introduced into the catalyst-containing vessel. The calorimetric and volumetric data were stored and analyzed by a special computer processing. The CO uptake at the monolayer is deduced from the amount of CO adsorbed with heats higher than $40\,kJ\,mol^{-1}$.

H_2 and CO uptakes were used to determine the metal dispersion, *D*, by assuming that either one hydrogen atom or one CO molecule is chemisorbed on one metal surface atom. The average particle size value, *d*, was calculated from the equations $d\ (nm) = 1.03/D$ for Pt and $d\ (nm) = 1.32/D$ for Ru [19].

The particle sizes distribution in bimetallic catalysts reduced at 573 K for 2 h under hydrogen were determined by transmission electron microscopy. Micrographs of the samples were obtained in a JEOL JEM-2000 FX transmission electron microscope at an accelerating voltage of 200 kV. The samples were ground with a mortar and then ultrasonically dispersed in *n*-butanol. A drop of this suspension was placed on a copper grid with a carbon support film and dried under infrared radiation.

2.4. n-Hexane reaction

The *n*-hexane reaction was carried out in a fixed bed quartz reactor (4 mm ID) at atmospheric pressure [20]. The weight of sample for each experiment was limited to keep conversion below 10%. Usually, a catalyst of 30 mg was loaded in the reactor. The *n*-hexane was fed into the reactor by bubbling a H_2 (20 ml min^{-1}) flow through a saturator-condenser maintained at 293 K (the molar ratio of H_2 to *n*-C_6H_{14} was 5.3). The catalyst was reduced in a 20 ml min^{-1} hydrogen flow at 750 K for 2 h and the reaction was carried out at the same temperature. The effluents of the reactor were analyzed by an on line gas chromatograph (Varian 3400) equipped with a thermal conductivity detector and a 30% DC-200 Chromosorb P-AW column. The conversion of *n*-hexane was calculated as $[\sum(iC_i/6)/(C_6 + \sum iC_i/6)] \times 100$ and the selectivity of products was evaluated as $(iC_i/\sum iC_i) \times 100$, where C_i is the molar concentration of product *i* and C_6 the molar concentration of *n*-hexane. The turnover frequency (TOF) of a catalyst was calculated as the number of *n*-hexane molecules converted per surface metal atom. The fragmentation factor of hydrogenolysis was defined as $\xi = \sum C_i/(\sum iC_i/6)$.

3. Results and discussion

3.1. Temperature-programmed reduction

Fig. 1 shows the TPR results of the series of Pt–Ru catalysts. It can be seen that only one peak appears at 388 K for the platinum catalyst in Fig. 1a. The hydrogen consumption corresponds to the reduction of the metal precursor from Pt^{4+} to Pt^0. On the other hand, the monometallic ruthenium catalyst shows two reduction peaks at 403 and 488 K. The two peaks can be assigned to the reduction reaction of $RuCl_3$ to the zero-valent state of Ru. The difference in reduction temperature can be a consequence of the metal precursor crystallite size. It is well known that bulk $RuCl_3$ reduces at higher temperatures than dispersed-supported $RuCl_3$ [21].

The Pt–Ru catalysts with different atomic ratios mainly show a peak of hydrogen consumption at ca. 423 K with a shoulder at ca. 473 K (Fig. 1b–d). The maximum of hydrogen consumption for the bimetallic samples is shifted to higher temperature (ca. 423 K) as the Ru loading increases in comparison with the pure Pt catalyst (Fig. 1a). The shift of the platinum reduction temperature by 35–45 K indicates a strong interaction between Pt and Ru atoms, probably because Pt and Ru are very close each other. Blanchard et al. reported identical results when the TPR of SiO_2 supported bimetallic Pt–Ru catalysts containing ca. 10 wt.% metal was studied. They attributed this result to the co-crystallization of platinum and ruthenium chlorides during the drying procedure of the preparation [22]. At temperatures exceeding 523 K the hydrogen consumption observed in TPR profiles

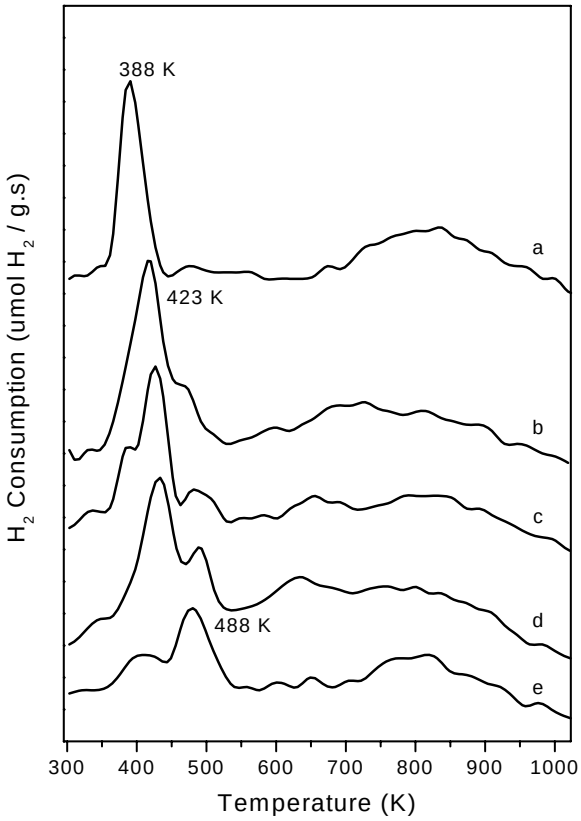

Fig. 1. TPR profiles of the different carbon supported Pt–Ru catalysts: (a) 2 wt.% Pt/XC72R; (b) 2 wt.% Pt–0.52 wt.% Ru/XC72R; (c) 2 wt.% Pt–1.03 wt.% Ru/XC72R; (d) 2 wt.% Pt–2.03 wt.% Ru/XC72R; (e) 2 wt.% Ru/XC72R.

is associated to the partial gasification of the support around the metallic particles since it is accompanied by CH_4 evolution [23].

3.2. Particle sizes and dispersion

From the TPR results it has been found that reduction at 573 K is sufficient to complete the transformation of the metal precursors to the zero-valent state for both Pt and Ru. Therefore, temperature (573 K) was chosen as standard reduction temperature for the samples. Table 1 presents the metallic dispersion, the average metal particle size determined by H_2 and CO chemisorption for the monometallic samples and by transmission electron microscopy for Pt–Ru catalysts.

The monometallic Pt catalyst shows the highest capacity for hydrogen adsorption and the highest metallic dispersion. While the Ru catalyst exhibits much lower adsorption ability for hydrogen than for CO. This fact may be due to the well-established character of activated process that exhibits the hydrogen on supported Ru particles [24,25]. For the three bimetallic catalysts, the H_2 uptake was sharply decreased by the increase of the Ru content, i.e., the surface ruthenium atoms are being underestimated. Therefore, for containing ruthenium catalysts the hydrogen uptake at room

Table 1
Metallic dispersion and average particle sizes of the Pt–Ru catalysts

Catalyst (ratio of Pt/Ru)	Chemisorption of H_2			Chemisorption of CO			TEM, d (nm)	Q_{ads} (kJ/mol)
	N_{ads} (μmol/g)	D (%)	d (nm)	N_{ads} (μmol/g)	D (%)	d (nm)		
2 wt.% Pt/XC72R	31.2	61	1.8	43.0	42	2.7		125
2 wt.% Pt–0.52 wt.% Ru/XC72R (2:1)	21.5	28		43.1	28		2.3	124
2 wt.% Pt–1.03 wt.% Ru/XC72R (1:1)	12.8	13		44.0	22		2.0	124
2 wt.% Pt–2.03 wt.% Ru/XC72R (1:2)	14.0	9		68.0	23		2.7	112
2 wt.% Ru/XC72R	4.2	4	27	63.5	32	3.9		109

temperature does not give a realistic estimation of the metal dispersion on the catalyst surface.

On the other hand, as can be inferred from Table 1, the capacity of adsorbed CO does not show a progressive correlation with the metal content. At the same time, the bimetallic catalysts with Pt/Ru ratios of 2:1 and 1:1 do not modify the CO uptake in comparison with the monometallic Pt sample and the bimetallic catalyst with a Pt/Ru ratio of 1:2 shows a moderate increase in the capacity of adsorption. Metal particle sizes calculated for the monometallic catalysts from the adsorption measurements indicate an average metal particle of 2 nm for the platinum catalyst and a particle size close to 4 nm for the ruthenium sample. To determine the metal particle size in the bimetallic catalysts, transmission electron microscopy has been proved to be a useful tool. The particle sizes distribution in Pt–Ru catalysts has been determined by directly measuring sizes of 200 particles in magnified TEM photographs (Figs. 2 and 3). The obtained histograms include the analysis of several parts of TEM photographs. The three catalysts with atomic ratios of Pt/Ru of 2:1, 1:1 and 1:2 present a high uniform dispersion of particle sizes and morphology with a mean diameter ranging from 2.0 to 2.7 nm. It is worthy to note that the evolution of CO uptakes over bimetallic catalysts does not parallel metal particle sizes determined by TEM. These effects may be attributed to the formation of a Pt–Ru alloy in where the CO/M adsorption stoichiometry is different to the value 1 assumed for monometallic catalysts.

X-ray diffraction patterns of the carbon supported catalysts did not give any diffraction peaks, corroborating that the bimetallic components are highly dispersed and the sizes of the metallic crystallites remain below the size limit of XRD detectability (4 nm).

3.3. Differential heats of adsorption

Direct adsorption microcalorimetric measurements provided accurate values of the adsorption heats, and also an energetic distribution of the surface sites as a function of the coverage is drawn. Fig. 4 exhibits the differential heats of CO adsorption as a function of the coverage. From Fig. 4 and the data in Table 1 it can been seen that the Pt catalyst, with initial differential heat of 125 kJ mol^{-1}, shows stronger CO adsorption sites than the pure Ru catalyst, with initial differential heat of 109 kJ mol^{-1}. It is worth noting that the three bimetallic catalysts with different Pt to Ru ratios display similar shapes of adsorption heats falling between the two monometallic samples before abrupt fall of the evolved heat to the physisorption field. When the atomic ratio of Pt to Ru is 2:1 to 1:1, the initial heats of CO adsorption (each sample, 124 kJ mol^{-1}) are similar to that of the pure Pt catalyst. The similarity of the initial differential heats of CO adsorption suggests that the CO is strongly adsorbed on some Pt atoms which are not modified by the presence of Ru. When the atomic ratios of Pt to Ru approaches 1:2, the initial heat of CO adsorption tends to resemble to that of pure Ru. Meanwhile, it can be found from Table 1 that the volumetric capacities of adsorbed CO for the bimetallic Pt–Ru catalysts are nearly half of those expected for the surface composed of two segregated metals, respectively. This can be explained if a CO adsorption stoichiometry on Pt–Ru alloyed phases different to that taking place on monometallic catalysts is assumed. From Fig. 4 it can be also seen that the energetic distribution curves of the surface sites of Pt–Ru alloys always fall below that of the pure Pt catalyst. Therefore, the Pt–Ru system chemisorbs CO in a lower extent and with a smaller strength. This is probably the reason why the Pt–Ru electrocatalysts have a better performance in PEMFCs and DMFCs as compared with monometallic Pt electrodes.

The surface composition and the bulk structure of this kind of catalysts are difficult to determine. Theoretical studies on clean surfaces composition of binary random alloys have been carried out on the base of ab initio calculations of the surface segregation energies of transition metal impurities at the most closed-packed surfaces of other transition metals [26,27]. Calculations made in the case of a Pt matrix indicate that a solute as Ru would tend to remain in the interior of the host and vice versa, in a Ru matrix Pt would tend to segregate to the surface [28]. Studies on the effect of CO adsorption on surface segregation for a $Pt_{50}Ru_{50}$ alloy indicates some segregation of Ru to the surface, but all the Ru sites are covered by CO while the adsorption energy of CO on Pt is reduced [28]. This effect could explain the different tendencies in H_2 and CO adsorption for bimetallic catalysts.

3.4. Selectivity of n-hexane reaction

Aiming at obtaining more information about the surface structure of the bimetallic Pt–Ru catalysts, the *n*-hexane

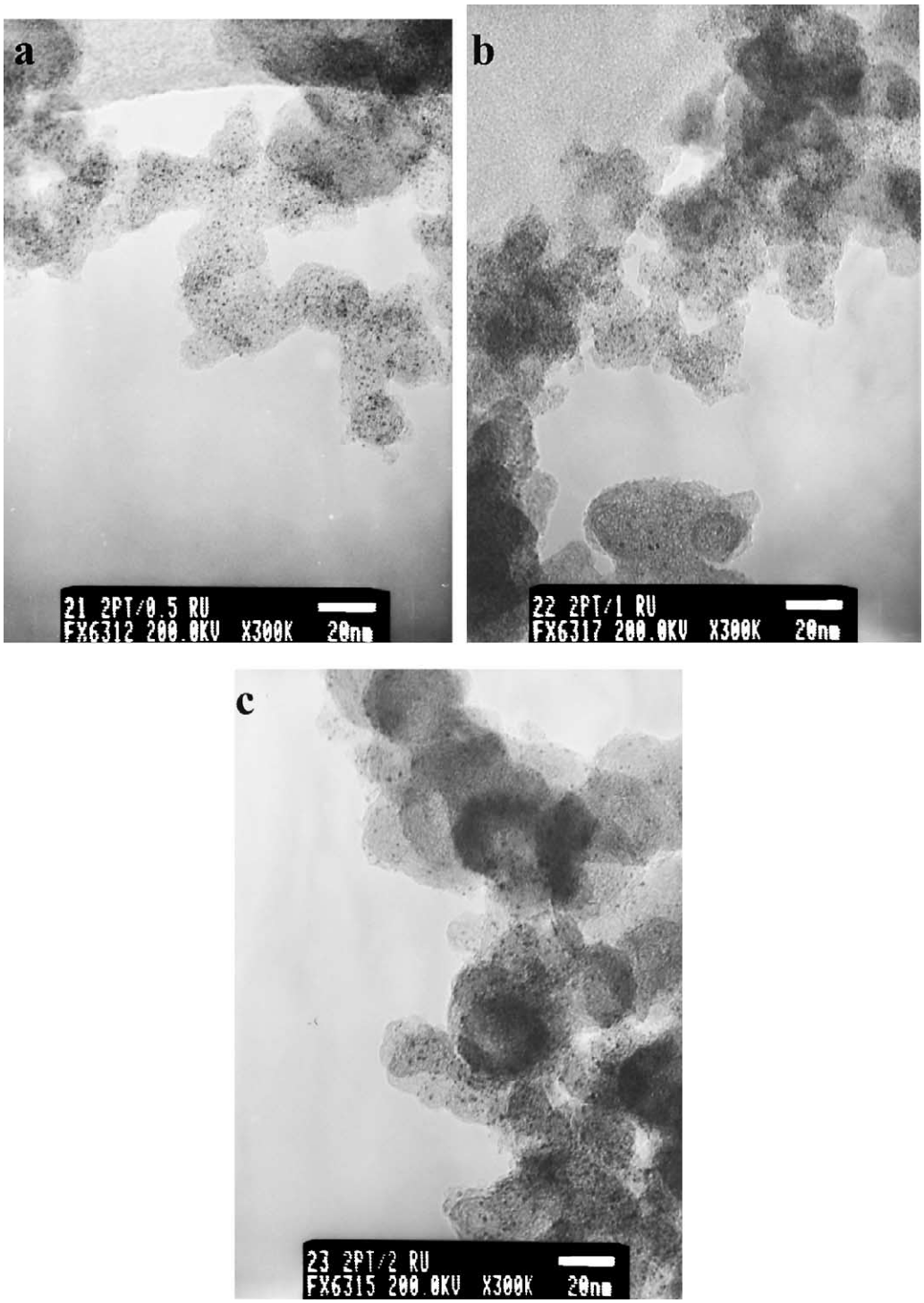

Fig. 2. TEM images and particle size distribution of the bimetallic Pt–Ru catalysts: (a) 2 wt.% Pt–0.52 wt.% Ru/XC72R; (b) 2 wt.% Pt–1.03 wt.% Ru/XC72R; (c) 2 wt.% Pt–2.03 wt.% Ru/XC72R.

reaction was carried out as test reaction. As hydrogenolysis and isomerization of hydrocarbons are structure-sensitive reactions [29], the selectivity pattern in the *n*-hexane conversion of the Pt–Ru catalysts can be informative about possible surface structure of the metallic aggregates and the coordination of the surface Pt atoms. The conversion of *n*-hexane was controlled below 10% and no significant deactivation occurred for each catalyst during the course of the reaction. The activity and selectivity of the catalysts after 2.5 h on-stream are listed in Table 2. The activity is expressed in turnover frequency, i.e. number of molecules of *n*-hexane transformed per unit time for one surface metal atom. It can be seen that the monometallic Ru is less active than the monometallic Pt, and that the turnover frequency were more

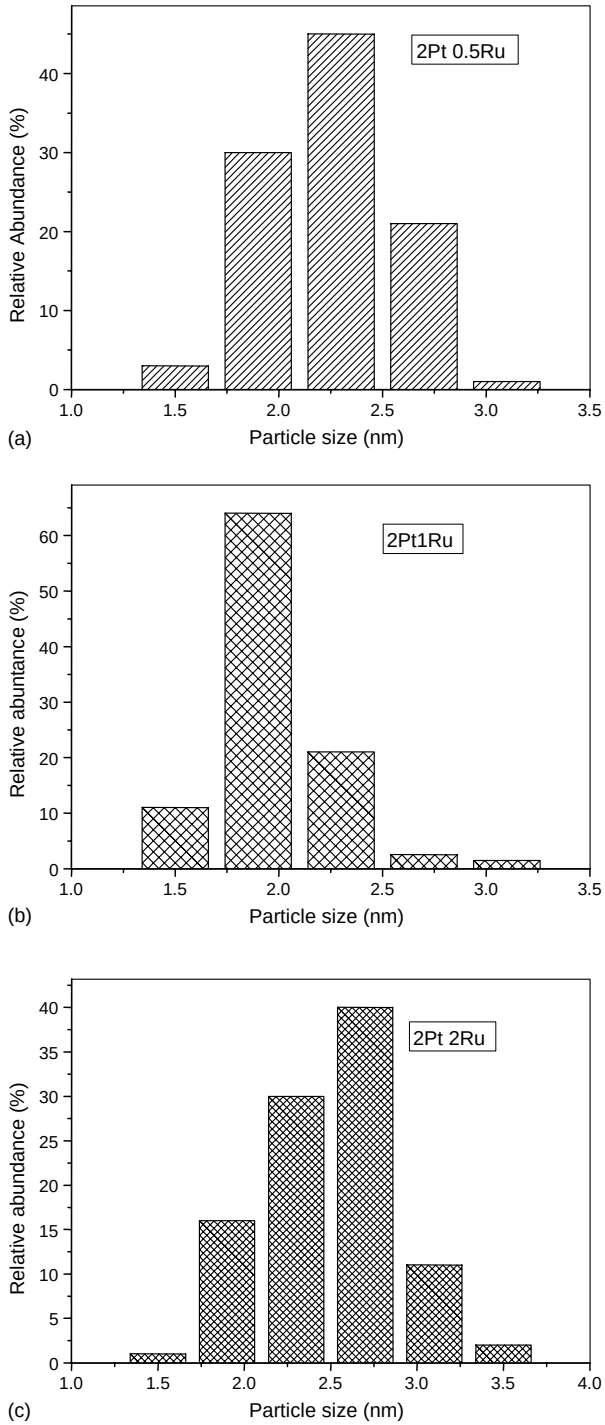

Fig. 3. Histograms of the particle size distribution in the bimetallic Pt–Ru catalysts: (a) 2 wt.% Pt–0.52 wt.% Ru/XC72R; (b) 2 wt.% Pt–1.03 wt.% Ru/XC72R; (c) 2 wt.% Pt–2.03 wt.% Ru/XC72R.

or less constant upon incorporation of an increasing amount of ruthenium.

The fragmentation factors, ξ, which characterize the depth of hydrogenolysis, represent the number of hydrocarbon fragments per decomposed molecule. The fragmentation factors for pure Pt and pure Ru catalysts seem very similar as shown in Table 2, and it is not changed by the ruthenium addition.

However, the selectivity pattern for *n*-hexane conversion in the two monometallics is quite different. Monometallic platinum gives low selectivity to hydrogenolysis (11%) the skeletal reactions of *n*-hexane being the main reactions. Monometallic ruthenium has a higher selectivity for hydrogenolysis conversion of *n*-hexane. These results agree with the more hydrogenolyzing character reported for the ruthenium [30]. The two monometallic catalysts differ also in the selectivity patterns towards six-carbon-atom products, i.e. isomers of hexane (iC_6), dehydrocyclation to methylcyclopentane (MCP) and aromatization to benzene (Bz). These selectivities are plotted in Fig. 5 as a function of the atomic percentage of Pt and Ru in the metallic phase. It can be found that the selectivity to isomerization considerably increases with the increasing amount of ruthenium for the Pt–Ru catalysts, while the selectivities to aromatization and dehydrocyclation to form MPC gradually decrease.

Two routes for skeletal reactions of alkanes have been described: the bond-shift mechanism (where a metallocyclobutane intermediate may exist) and the cyclic mechanism, where a cyclopentane intermediate is postulated [31]. The bond-shift mechanism in addition to isomerization gives also the hydrogenolysis reaction being this latter the preferred one. On platinum catalysts the cyclic mechanism prevails over the bond-shift producing isomerization, dehydrogenative C_5-cyclation and aromatization (via C_5-cycle enlargement) [32] and it seems that the selectivity pattern of our monometallic Pt catalysts support this route of reaction. It has been showed that the cyclic intermediate is flatly chemisorbed on the platinum surface requiring ensembles of platinum atoms of certain size and disposition [33,34]. Therefore, the variation in the selectivity for the Pt–Ru catalysts with respect to the monometallic Pt may be predominantly caused by geometric effects. Introduction of lowly active component (Ru) into highly active pure Pt catalyst may cause disruption of the Pt ensembles hindering the formation of the cyclic intermediate. For the 2 wt.% Pt–0.52 wt.% Ru catalyst, the Pt ensemble of active sites is still bigger enough to provide a set of Pt atoms (six or five atoms) for physical adsorption of *n*-hexane which lies parallel to the surface of atoms. The selectivity for aromatization is slightly lower than that of the pure Pt catalyst. With increasing Ru, the mean size of the Pt ensemble becomes more and more smaller and the distances between active sites enlarge. Therefore, the ensembles composed of six or five Pt atoms for catalytic adsorption of *n*-hexane hardly remain so that the selectivity of MCP and Bz gradually drop down.

On the contrary, the selectivity to isomerization (six-carbon-atom products others that MCP and Bz) sharply increases with Ru content in Fig. 5. It can be explained by the bond-shift mechanism [35] which involves formation of an intermediate adsorbed by a single bond, that is, one carbon atom of *n*-hexane adsorbs on the active site of one

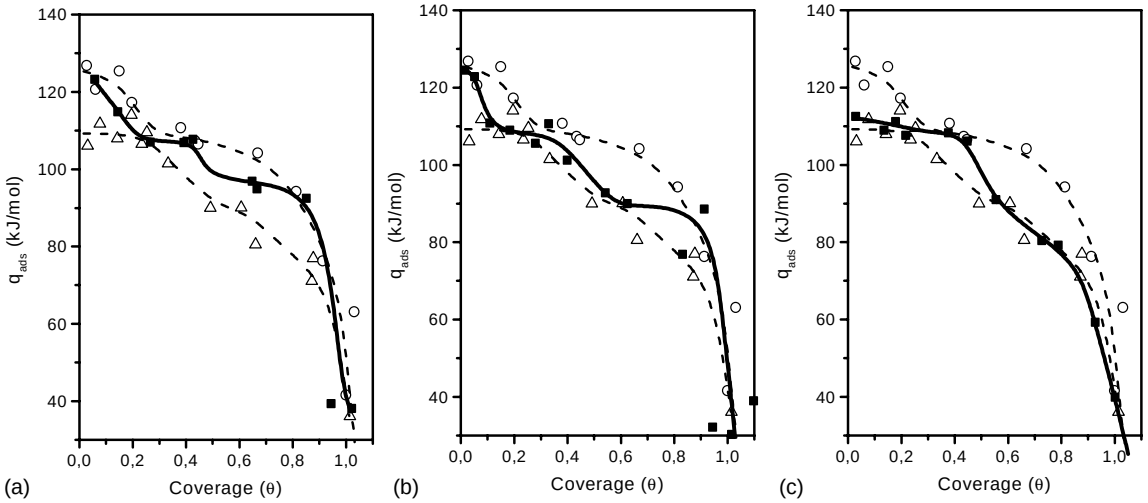

Fig. 4. Differential heats of CO adsorption at 330 K as a function of surface coverage for catalysts: (○) 2 wt.% PtXC72R; (△) 2 wt.% RuXC72R; (■) Pt–Ru/XC72R ((a) 2 wt.% Pt–0.52 wt.% Ru/XC72R; (b) 2 wt.% Pt–1.03 wt.% Ru/XC72R; (c) 2 wt.% Pt–2.03 wt.% Ru/XC72R).

Table 2
Catalytic properties of the different catalysts for the conversion of *n*-hexane[a]

Catalyst	Conversion (%)	TOF[b] (s^{-1})	Selectivity of product (%)				ξ
			C_1–C_5	iC_6	MCP	Bz	
2 wt.% Pt/XC72R	10.2	0.19	11	41	16	32	3.0
2 wt.% Pt–0.52 wt.% Ru/XC72R	9.1	0.16	11	44	17	28	3.4
2 wt.% Pt–1.03 wt.% Ru/XC72R	9.0	0.16	9	61	14	16	3.3
2 wt.% Pt–2.03 wt.% Ru/XC72R	9.8	0.11	10	66	11	13	3.0
2 wt.% Ru/XC72R	3.2	0.04	22	57	7	14	3.1

[a] Reaction temperature, 750 K; H_2/*n*-C_6H_{14} = 5.3:1; time on-stream 2.5 h.
[b] TOF calculated as the number of *n*-hexane molecules converted per surface metal atom (determined by CO chemisorption).

Pt atom and then removes one hydrogen atom to produce a σ-alkyl adsorbed species which promote skeletal isomerization without cycle formation. These changes in the selectivity pattern in *n*-hexane conversion to six-carbon-atom products parallel those previously reported on the diluting effect of the a second metal, such as, Re and Au [36,37].

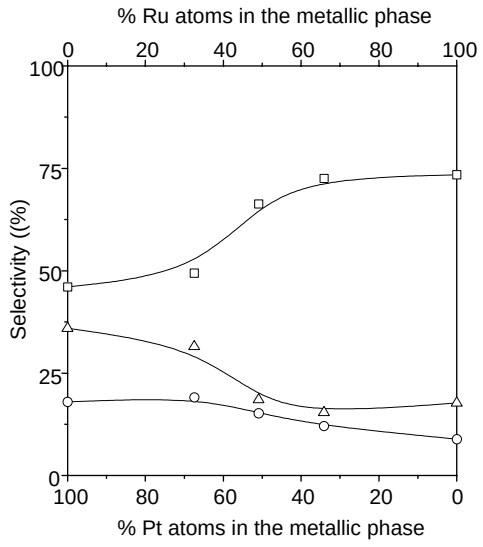

Fig. 5. Selectivities distribution towards C_6 products: (□) hexane isomers (iC_6); (○) methylcyclopentane (MCP); (△) benzene (Bz). Reaction temperature, 750 K; H_2/*n*-C_6H_{14} = 5.3:1; time on-stream 2.5 h.

Comparison of the selectivity patterns in *n*-hexane reaction for the different catalysts allow to conclude: (1) pure Pt showed mainly cyclic isomerization and aromatization due to bigger Pt surface ensembles; (2) Pt–Ru alloy presented skeletal isomerization by the diluting effect of the added Ru metal to Pt which reduces the ensemble sizes.

4. Conclusion

A series of highly dispersed Pt/Ru alloyed catalysts with different Pt:Ru atomic ratios and uniform particle sizes were prepared by co-impregnation of carbon with $RuCl_3 \cdot xH_2O$ and $H_2PtCl_6 \cdot 6H_2O$. The TPR results on these samples revealed a strong interaction between both metals indicating that Pt and Ru are alloyed. The selectivity patterns obtained for a structure-sensitive reaction, *n*-hexane conversion, indicate that the Pt/Ru alloys are responsible for the high selectivity to skeletal isomerization without cycle intermediate formation. Microcalorimetry results show the energetic distribution of the surface sites of the Pt–Ru alloys, in which the CO adsorption energy decrease for differently atomic ratios of Pt–Ru catalysts in comparison to the pure Pt

catalyst. This fact is probably the reason why the Pt–Ru alloyed electrocatalysts have a better performance in PEMFCs and DMFCs as compared with monometallic Pt electrodes.

Acknowledgements

This work was supported by the MCyT under project MAT 2002-04189-C02 and by the MAE-AECI, project 2002CN0005. We are also grateful to the Microscopy Centre "Luis Bru" of the Complutense University of Madrid (UCM) for the TEM analysis.

References

[1] S.D. Lin, T.-C. Hsiao, J.-R. Zhang, A.S. Lin, J. Phys. Chem. B 103 (1999) 97.
[2] H.A. Gastiger, N. Markovic, P.N. Ross Jr., J. Phys. 99 (1995) 16757.
[3] A.S. Arico, S. Srinivasan, V. Antonucci, Fuel Cells 1 (2) (2001) 1.
[4] S. Wasmus, A. Kuver, J. Electroanal. Chem. 461 (1999) 14.
[5] M. Watanabe, M. Uchida, S. Motoo, J. Electroanal. Chem. 229 (1987) 395.
[6] S. Lee, K. Park, J. Choi, B. Kwon, J. Electrochem. Soc. 149 (10) (2002) A1299.
[7] M.T. Paffet, G.J. Beery, S. Gottesfeld, J. Electrochem. Soc. 135 (1998) 1434.
[8] A. Freund, J. Lang, T. Lehman, K.A. Starz, Catal. Today 27 (1996) 279.
[9] M. Watanabe, S. Motoo, J. Electroanal. Chem. 60 (1975) 275.
[10] H.N. Dinh, X. Ren, F.H. Garzon, P. Zelenay, J. Electroanal. Chem. 491 (2000) 222.
[11] W. Li, C. Liang, J. Qiu, W. Zhou, H. Han, Z. Wei, G. Sun, Q. Xin, Carbon 40 (2002) 787.
[12] H.G. Petrow, R.J. Allen, US Patent 3,992,331 (1976).
[13] T.J. Schmidt, M. Noeske, H.A. Gasteiger, R.J. Behm, P. Britz, W. Brijoux, H. Bonnemann, Langmuir 13 (1997) 2591.
[14] T.H. Galow, A.K. Boal, V.M. Rotello, Adv. Mater. 12 (2000) 576.
[15] V. Radmilovic, H.A. Gasteiger, P.N. Ross Jr., J. Catal. 154 (1995) 98.
[16] B. Bachiller-Baeza, A. Guerrero-Ruiz, I. Rodriguez-Ramos, Appl. Catal. A: Gen. 192 (2000) 289.
[17] I. Rodriguez-Reinoso, I. Rodriguez-Ramos, C. Moreno-Castilla, A. Guerrero-Ruiz, J.D. Lopez-Gonzalez, J. Catal. 99 (1986) 171.
[18] A. Guerrero-Ruiz, A. Maroto-Valiente, M. Cerro-Alarcón, B. Bachiller-Baeza, I. Rodríguez-Ramos, Topics Catal. 19 (3–4) (2002) 303.
[19] J.R. Anderson, Structure of Metallic Catalysts, Academic Press, 1975, p. 295.
[20] A. Guerrero-Ruiz, B. Bachiller-Baeza, P. Ferreira-Aparicio, I. Rodriguez-Ramos, J. Catal. 171 (1997) 374.
[21] G.C. Bond, R.R. Rajaram, Appl. Catal. 27 (1989) 379.
[22] G. Blanchard, H. Charcosset, M.T. Chenebaux, M. Primet, Proceedings of the 2nd International Symposium on Scientific Bases got the Preparation of Heterogenous Catalysts, Louvain La-Neuve, Belgium, 1978, p. B8.
[23] A. Guerrero-Ruiz, A. Sepulveda-Escribano, I. Rodriguez-Ramos, Appl. Catal. A: Gen. 120 (1994) 71.
[24] M. Uchida, A.T. Bell, J. Catal. 60 (1979) 204.
[25] A. Guerrero-Ruiz, P. Badenes, I. Rodríguez-Ramos, Appl. Catal. A: Gen. 173 (1998) 313.
[26] A.V. Ruban, H.L. Skriver, J.K. Norskov, Phys. Rev. B 59 (15) (1999) 990.
[27] A. Christensen, A.V. Ruban, P. Stoltze, K.W. Jacobsen, H.L. Skriver, J.K. Norskov, Phys. Rev. B 56 (1977) 5822.
[28] E. Christoffersen, P. Liu, A. Ruban, H.L. Skriver, J.K. Norskov, J. Catal. 199 (2001) 123.
[29] Z. Paál, P. Tetenyi, in: G.C. Bond, G. Webb (Eds.), Specialist Periodical Reports: Catalysis, vol. 5, Royal Society of Chemistry, London, 1982, p. 80.
[30] B. Coq, A. Bittar, F. Figueras, Appl. Catal. 59 (1990) 103.
[31] G.C. Bond, Chem. Soc. Rev. 20 (1991) 441.
[32] Z. Paal, H. Groeneweg, J. Paal-Lukacs, J. Chem. Soc., Faraday Trans. 86 (1990) 3159.
[33] Z. Paal, P. Tetenyi, Nature 267 (1977) 234.
[34] T.G. Olfer'eva, O.V. Bragin, A.L. Liberman, Izv. Akad. Nauk. SSSR, Ser. Khim. (1970) 1517.
[35] F.G. Gault, Advances in Catalysis, vol. 30, Academic Press, New York, 1981, p. 1.
[36] J.R.H. van Schaik, R.P. Dessing, V. Ponec, J. Catal. 38 (1975) 273.
[37] C. Bolivar, H. Charcosset, R. Frety, M. Prlmet, L. Tournayan, J. Catal. 45 (1976) 163.